Available online at www.sciencedirect.com
ScienceDirect
Journal of Organometallic Chemistry 692 (2007) 1584–1592
Journal of Organometallic Chemistry
www.elsevier.com/locate/jorganchem

1-D Polymeric divalent metal *m*-ferrocenylbenzoates: Structures, NLO and electrochemical properties

Jinpeng Li [a], Yinglin Song [b], Hongwei Hou [a,*], Mingsheng Tang [a], Yaoting Fan [a], Yu Zhu [a]

[a] *Department of Chemistry, Zhengzhou University, Henan 450052, PR China*
[b] *Department of Physics, Harbin Institute of Technology, Heilongjiang 150001, PR China*

Received 20 October 2006; received in revised form 1 December 2006; accepted 12 December 2006
Available online 20 December 2006

Abstract

Three 1-D metal–organic polymers containing *m*-ferrocenylbenzoate components: $\{[Pb(\mu_2\text{-}\eta^2\text{-}OOCH_4C_6Fc)_2]\cdot(CH_3OH)_2\}_n$ (**1**), $[Zn(OOCH_4C_6Fc)_2(bpe)]_n$ (**2**) and $[Mn(\eta^2\text{-}OOCH_4C_6Fc)_2(4,4'\text{-}bpy)]_n$ (**3**) were synthesized and structurally characterized. In polymer **1**, each $m\text{-}FcC_6H_4COO^-$ anion adopts a tridentate fashion, bridging the central Pb(II) ions to form a 1-D chain. Polymers **2** and **3** give similar zigzag chain structures. Their third-order NLO properties were investigated with 532 nm laser pulses of 8 ns duration by *Z*-scan experiment in DMF solution. All of the polymers exhibit good NLO refractive properties with self-focusing behaviors. The third-order NLO refractive indexes n_2 are 2.44×10^{-11} esu for **1**, 2.33×10^{-11} esu for **2**, and 2.10×10^{-11} esu for **3**, respectively. Through quantum chemistry calculations, we conclude that the nonlinear refractive behaviors of the three polymers mainly come of the ferrocenyl units and organic adjuvant ligands; Mn(II) ions and Pb(II) ions have also some influence on NLO properties. The solution-state differential pulse voltammetrys indicate that the half-wave potential of the ferrocenyl moiety in **3** has slightly higher value than those of **1** and **2**. This may be because the HOMO orbitals in **1** and **2** are located in the $m\text{-}FcC_6H_4COO^-$ groups, while in **3** the HOMO orbital is located in the $m\text{-}FcC_6H_4COO^-$ and Mn(II)groups, the charge transitions of the metal cores may play an important role in the change of the Fe(II)/Fe(III) oxidation potential of **3**, so the Fe(II) centers of **1** and **2** are more easily oxidized to Fe(III) centers than that of **3**.

Keywords: Ferrocene; Electrochemistry; Nonlinear optical properties; Quantum calculation

1. Introduction

Tempted by potential application of nonlinear optical devices, much effort has been made in recent years in the design and synthesis of new molecules with large macroscopic optical nonlinearities [1] and in demonstrating their logic operation, optical switching, optical communication, optical limiting effect, etc. [2]. Within this field, ferrocene-containing complexes are currently attracting a great deal of attention [3–5]. Ferrocenyl complexes consist of ferrocenyl units, metal ions, or organic adjuvant ligands, each of which may make an important contribution to optical nonlinearity of ferrocenyl complexes. Rich electronic ferrocenyl units and organic adjuvant ligands containing π-conjugated system can enhance the delocalization of π-electron cloud over the whole chain [6] and then boost up the molecular NLO properties [7]. The incorporation of transition metal ions in metal–organic complexes introduces more sublevels into the energy hierarchy, which permits more allowed electronic transitions to take place and enhances the NLO effects. Therefore, ferrocenyl complexes have been expected to be one of the new candidates for nonlinear optical materials, and it has been found that ferrocenyl metal–organic complexes exhibit good third-order NLO effects [5,8].

Furthermore, from the viewpoint of constructing functional compounds, the incorporation of the ferrocene moiety into the metal–organic frameworks provides a good select of preparing new functional materials with

* Corresponding author. Tel./fax: +86 371 67761744.
E-mail address: houhongw@zzu.edu.cn (H. Hou).

0022-328X/$ - see front matter © 2006 Elsevier B.V. All rights reserved.
doi:10.1016/j.jorganchem.2006.12.010

unique features. Additionally, the utilization of organic adjuvant ligands containing π-conjugated system (4,4′-bpy, bpe, etc.) can benefit the attachment of ferrocenyl units to polymeric chains [9], and therefore extend the π-conjugation length of complexes which is one of many features to increase molecular NLO susceptibility $\chi^{(3)}$ values [10]. These prompt us to utilize adjuvant ligands to prepare more novel metal–organic polymers containing ferrocene groups and study their NLO properties. However, to our knowledge, there were few reports [8] on the third-order NLO properties of ferrocenyl metal–organic polymers.

On the other hand, although the great progress made in the field of NLO materials, the crucial influence factors of forming better NLO materials still remain unclear. It decelerates the speed of further development of nonlinear optics. Increasing researchers are trying to reveal the influence factors concerning NLO properties in order to establish some well-defined guidelines or models for synthesizing better third-order species [6,11]. In our previous work [11d], we have reported that the frontier molecular orbital corresponds to the delocalization of the π-electron cloud and such cloud is generally suggested as the origin of NLO properties of metal complexes. To further investigate the influence factors concerning NLO properties and search for new potential third-order NLO materials, we utilized sodium *m*-ferrocenylbenzoate to design and synthesize three novel one-dimensional polymers containing different metal ions: $\{[Pb(\mu_2\text{-}\eta^2\text{-}OOCH_4C_6Fc)_2]\cdot(CH_3OH)_2\}_n$ (**1**), $[Zn(OOCH_4C_6Fc)_2(bpe)]_n$ (**2**) and $[Mn(\eta^2\text{-}OOCH_4C_6Fc)_2(4,4'\text{-bpy})]_n$ (**3**). As expected, these polymers all present good third-order NLO properties. By quantum chemistry study, we illustrate that metal ions in polymers **1**, **2** and **3** have different influence on third-order NLO properties and the nonlinear refractive behaviors of three polymers mainly come of the ferrocenyl units and organic adjuvant ligands. Their electrochemical properties were also investigated.

2. Experimental

2.1. General Information and physical techniques

All chemicals were of reagent grade quality obtained from commercial sources and used without further purification. Carbon, hydrogen and nitrogen analyses were carried out on a Carlo-Reba 1106 elemental analyzer. IR data were recorded on a Nicolet NEXUS 470-FTIR spectrophotometer with KBr pellets in the 400–4000 cm^{-1} region. UV–vis spectra were recorded, ranging from 240 to 700 nm, on a JASCO V-550 ultraviolet–visible spectrophotometer. *m*-Ferroceneylbenzoic acid and its sodium salt were prepared according to the literature method [12]. Cyclic voltammogram and differential pulse voltammetry studies were recorded with a CHI650 electrochemical analyzer utilizing the three-electrode configuration of a Pt working electrode, a Pt auxiliary electrode, and a commercially available saturated calomel electrode as the reference electrode with a pure N_2 gas inlet and outlet. The measurements were performed in DMF solution containing tetrabutyl ammonium perchlorate (n-Bu_4NClO_4) (0.1 mol dm^{-3}) as supporting electrolyte, with has a 50 ms pulse width and a 20 ms sample width. The potential was scanned from 0 to +1.0 V at a scan rate of 20 mV s^{-1}.

2.2. Synthesis of $\{[Pb(\mu_2\text{-}\eta^2\text{-}OOCH_4C_6Fc)_2]\cdot(CH_3OH)_2\}_n$ (1)

$Pb(OAc)_2\cdot 3H_2O$ (19.0 mg, 0.05 mmol) was dissolved in 5 ml CH_3OH. A 4 ml CH_3OH solution of *m*-FcC_6H_4COONa (32.8 mg, 0.1 mmol) was added dropwise to the former mixture at r.t. After several days, red X-ray quality single crystals were obtained (20 mg). Anal. Calc. for $C_{36}H_{34}Fe_2O_6Pb$: C, 49.01; H, 3.90. Found: C, 48.79; H, 3.97%. IR spectra (KBr cm^{-1}): 3444 (s), 1599 (s), 1553 (s), 1464 (m), 1396 (s), 1271 (m), 1130.28 (m), 1104 (m), 1077 (m), 1007 (m), 815 (m), 773 (m), 719 (m), 692 (m), 652 (m), 499 (m).

2.3. Synthesis of $[Zn(OOCH_4C_6Fc)_2(bpe)]_n$ (2)

The ligand *m*-FcC_6H_4COONa (32.8 mg, 0.1 mmol) in 5 mL of CH_3OH was added dropwise to a solution of bpe (9.1 mg, 0.05 mmol) (bpe = 1,2-bis(4-pyridyl)thane) and $Zn(OAc)_2\cdot 2H_2O$ (11.0 mg, 0.05 mmol) in 5 mL of CH_3OH. Red single crystals were obtained after the reaction mixture was put in the dark for two week. Yield: 54%. Anal. Calc. for $C_{46}H_{36}Fe_2N_2O_4Zn$: C, 64.41; H, 4.20; N, 3.31. Found: C, 64.22; H, 4.31; N, 3.40%. IR (cm^{-1}, KBr): 3428 (s), 3095 (s), 1613 (s), 1567 (s), 1379 (s), 1263 (m), 1213 (m), 1104 (m), 1070 (m), 1024.32(m), 827.51(m), 555 (m), 495 (m).

2.4. Synthesis of $[Mn(\eta^2\text{-}OOCH_4C_6Fc)_2(4,4'\text{-bpy})]_n$ (3)

The ligand *m*-FcC_6H_4COONa (32.8 mg, 0.1 mmol) in 5 mL of CH_3OH was added dropwise to a solution of 4,4′-bpy (7.8 mg, 0.05 mmol) and $Mn(OAc)_2\cdot 2H_2O$ (13.4 mg, 0.05 mmol) in 5 mL of CH_3OH. Red single crystals were obtained after the reaction mixture was put in the dark for two week. Yield: 46%. Anal. Calc. for $C_{44}H_{34}Fe_2MnN_2O_4$: C, 64.30; H, 4.13; N, 3.41. Found: C, 64.24; H, 4.18; N, 3.38%. IR (cm^{-1}, KBr): 3429 (m), 3098 (m), 1600 (s), 1648 (s), 1490 (m), 1406 (s), 1272 (m), 1220 (m), 1131 (m), 1105 (m), 813 (m), 496 (m).

Caution! *Although no problems were encountered in this work, the salt perchlorates are potentially explosive. They should be prepared in small quantities and handled with care.*

2.5. Crystal structure determination

A crystal suitable for X-ray determination was mounted on a glass fiber. All data were collected at

room temperature on a Rigaku RAXIS-IV imaging plate area detector with graphite monochromated Mo-Kα radiation ($\lambda = 0.71073$ Å). The structures were solved by direct methods and expanded with Fourier techniques. The non-hydrogen atoms were refined anisotropically. Hydrogen atoms were included but not refined. The final cycle of full-matrix least-squares refinement was based on observed reflections and variable parameters. All calculations were performed with the SHELXL-97 crystallographic software package [13]. Table 1 shows crystallographic crystal data and processing parameters for polymers **1**–**3**, and Table 2 lists their selected bond lengths and bond angles.

2.6. Nonlinear optical measurements

A DMF solution of polymer **1** (**2** or **3**) was placed in a 1-mm quartz cuvette for NLO measurements, respectively. The NLO properties were measured as described in the literature [14].

2.7. Computational details

All computations were performed using the Gaussian 03 suite of programs and gradient corrected density functional theory using the B3LYP functional [15,16].

3. Results and discussion

3.1. Description of crystal structures

3.1.1. Crystal structure of $\{[Pb(\mu_2\text{-}\eta^2\text{-}OOCH_4C_6Fc)_2]\cdot(CH_3OH)_2\}_n$ (1)

The chain structure of polymer **1** is depicted in Fig. 1, from which we can see that each *m*-$FcC_6H_4COO^-$ anion adopts a tridentate fashion bridging the central Pb(II) ions to form a 1-D chain. The geometry around each Pb(II) ion can be described as a tent conformation. The four oxygen atoms (O1, O2, O1A, O2A) form the bottom of the tent, where the four O atoms are almost coplanar and atoms O1, O2 are from one *m*-$FcC_6H_4COO^-$ unit and O1A and O2A are from another *m*-$FcC_6H_4COO^-$ unit. O2B and O2C from two different *m*-$FcC_6H_4COO^-$ units form the top beam, the Pb atom locates within the middle portion of the top beam. The Pb–O bond distances are in the range of 2.510(6)–2.688(6) Å. The bond angles around Pb1 vary from 51.14° to 162.7°. The Pb(II) ions are not in a straight line: the adjacent Pb ⋯ Pb separation is 4.286(1) Å and Pb ⋯ Pb ⋯ Pb angle is 137.9°. The dihedral angles between planes Pb1B–O3B–Pb1–O3 and Pb1A–O2A–Pb1–O2 are 51.8, and the dihedral angles between planes C27–O4–Pb1–O3 and C13–O1–Pb1–O2 (the mean deviation from the plane both are 0.0023 Å)

Table 1
Crystal data and structure refinement for polymers **1**–**3**

Polymers	**1**	**2**	**3**
Formula	$C_{36}H_{34}Fe_2O_6Pb$	$C_{46}H_{36}Fe_2N_2O_4Zn$	$C_{44}H_{34}Fe_2MnN_2O_4$
fw	881.52	857.84	821.37
Temperature (K)	291(2)	291(2)	291(2)
Wavelength (Å)	0.71073	0.71073	0.71073
Crystal system	Monoclinic	Monoclinic	Monoclinic
Space group	*C*2/*c*	*C*2/*c*	*C*2/*c*
a (Å)	41.192(8)	28.020(6)	29.131(6)
b (Å)	10.123(2)	7.7307(15)	7.5343(15)
c (Å)	8.0021(16)	18.779(4)	16.441(3)
α (°)	90	90	90
β (°)	98.92(3)	106.02(3)	106.67(3)
γ (°)	90	90	90
V (Å^3)	3296.2(11)	3910.0(13)	3506.4(12)
z	4	4	4
D_c (g cm^{-3})	1.776	1.457	1.556
Absolute coefficient (mm^{-1})	6.008	1.387	1.220
F(000)	1728	1760	1684
Crystal sizes (mm)	0.20 × 0.18 × 0.16	0.20 × 0.18 × 0.16	0.20 × 0.18 × 0.16
θ Range for data collection (°)	2.07–27.59	1.51–25.00	1.44–27.53
Index ranges	$-51 \leqslant h \leqslant 52$, $-12 \leqslant k \leqslant 0$, $-9 \leqslant l \leqslant 9$	$-8 \leqslant h \leqslant 33$, $-9 \leqslant k \leqslant 8$, $-22 \leqslant l \leqslant 21$	$-36 \leqslant h \leqslant 9$, $-9 \leqslant k \leqslant 9$, $-18 \leqslant l \leqslant 19$
Reflections collected/unique	6131/3407	4705/2827	5564/3285
Data/restraints/parameters	3407/0/207	2827/0/254	3285/0/241
Goodness-of-fit on F^2	1.097	1.047	1.059
Final *R* indices [$I > 2\sigma(I)$]	$R1 = 0.0494$	$R1 = 0.0584$	$R1 = 0.0454$
R Indices (all data)	$wR2 = 0.1278$ $R1 = 0.0579$ $wR2 = 0.1345$	$wR2 = 0.0959$ $R1 = 0.1143$ $wR2 = 0.1084$	$wR2 = 0.0940$ $R1 = 0.0862$ $wR2 = 0.1050$

Table 2
Selected bond lengths (Å) and angles (°) for polymers **1**–**3**

Polymer ***1***[a]			
Pb(1)–O(2)	2.510(6)	Pb(1)–O(2)#1	2.510(6)
Pb(1)–O(1)	2.575(5)	Pb(1)–O(1)#1	2.575(5)
Pb(1)–O(2)#2	2.687(6)	Pb(1)–O(2)#3	2.688(6)
O(2)–Pb(1)#3	2.687(6)	O(2)#2-Pb(1)–O(2)#3	162.7(3)
O(2)–Pb(1)–O(2)#1	78.6(3)	O(2)–Pb(1)–O(1)	51.14(17)
O(2)#1-Pb(1)–O(1)	72.90(19)	O(2)–Pb(1)–O(1)#1	72.90(19)
O(2)#1-Pb(1)–O(1)#1	51.14(17)	O(1)–Pb(1)–O(1)#1	106.9(2)
O(2)–Pb(1)–O(2)#2	126.29(17)	O(2)#1-Pb(1)–O(2)#2	68.9(2)
O(1)–Pb(1)–O(2)#2	78.39(19)	O(1)#1-Pb(1)–O(2)#2	112.33(19)
O(2)–Pb(1)–O(2)#3	68.9(2)	O(2)#1-Pb(1)–O(2)#3	126.29(17)
O(1)–Pb(1)–O(2)#3	112.33(19)	O(1)#1-Pb(1)–O(2)#3	78.39(19)
Polymer ***2***[b]			
Zn(1)–O(1)	1.982(4)	Zn(1)–O(1)#1	1.982(4)
Zn(1)–N(1)	2.078(4)	Zn(1)–N(1)#1	2.078(4)
O(1)–Zn(1)–O(1)#1	122.8(3)	O(1)–Zn(1)–N(1)	118.32(18)
O(1)#1-Zn(1)–N(1)	100.13(18)	O(1)–Zn(1)–N(1)#	100.13(18)
O(1)#1-Zn(1)–N(1)#1	118.32(18)	N(1)–Zn(1)–N(1)#1	94.5(2)
Polymer ***3***[c]			
Mn(1)–O(1)	2.208(3)	Mn(1)–O(1)#1	2.208(3)
Mn(1)–N(1)#1	2.246(2)	Mn(1)–N(1)	2.246(2)
Mn(1)–O(2)	2.246(3)	Mn(1)–O(2)#1	2.246(3)
O(1)-Mn(1)–O(1)#1	133.69(14)	O(1)-Mn(1)–N(1)#1	90.54(9)
O(1)#1-Mn(1)–N(1)#1	122.67(11)	O(1)-Mn(1)–N(1)	122.67(11)
O(1)#1-Mn(1)–N(1)	90.54(9)	N(1)#1-Mn(1)–N(1)	91.39(13)
O(1)-Mn(1)–O(2)	58.42(9)	N(1)#1-Mn(1)–O(2)	145.09(10)
N(1)-Mn(1)–O(2)	92.89(9)	O(1)-Mn(1)–O(2)#1	91.93(11)
O(1)#1-Mn(1)–O(2)#1	58.42(9)	N(1)#1-Mn(1)–O(2)#1	92.89(9)
N(1)-Mn(1)–O(2)#1	145.09(10)	O(2)-Mn(1)–O(2)#1	102.92(14)

[a] Symmetry transformations used to generate equivalent atoms in **1**: #1 $-x+1, y, -z+1/2$ #2 $x, -y+1, z-1/2$ #3 $-x+1, -y+1, -z+1$.
[b] Symmetry transformations used to generate equivalent atoms in **2**: #1 $-x, y, -z+1/2$ #2 $-x, -y, -z+1$.
[c] Symmetry transformations used to generate equivalent atoms in **3**: #1 $-x, y, -z+1/2$ #2 $-x, -y+2, -z$.

are 76.5°. Interestingly, the Pb1–O2–Pb1A–O2B ring is similar to those of the reported Pb-carboxylate polymers [8,9c], in which carboxylate ligands are FcCH=CHCOOH and $FcC(CH_3)$=CHCOOH, respectively. It has been reported that the ring's structure of a Pb-carboxylate compound depends strongly on the size of the carboxylate substituent [17]. In addition, the one-dimensional [Pb(μ_2-η^2-$OOCH_4C_6Fc)_2$] chain extends along the *c*-direction. Viewing along *c*-axis, ferrocene fragments are located along both sides of the one-dimensional chains (Fig. 1), and they arrange alternately along this chain. {[Pb(μ_2-η^2-$OOCH_4C_6Fc)_2$]·$(CH_3OH)_2$}$_n$ chains pack each other by intermolecular interactions. Also it should be pointed out that the dihedral angle between the phenyl ring's plane and the Cp ring's plane of one *m*-$FcC_6H_4COO^-$ unit is 11.1°.

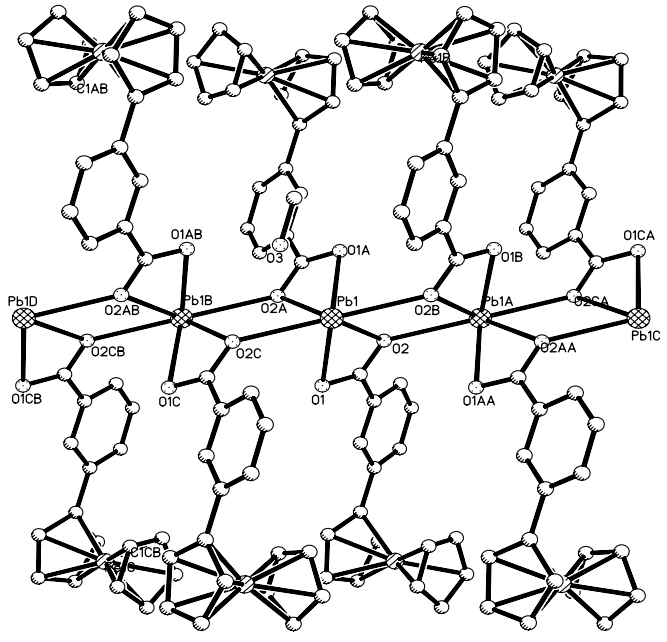

Fig. 1. Perspective view of the 1-D chain structure of {[Pb(μ_2-η^2-$OOCH_4C_6Fc)_2$]·$(CH_3OH)_2$}$_n$ with only the heteroatoms labeled.

3.1.2. Crystal structure of $[Zn(OOCH_4C_6Fc)_2(bpe)]_n$ (**2**)

Polymer **2** gives a one-dimensional zigzag chain structure (Fig. 2). It crystallizes in the space group *C*2/*c* as polymer **1**. In the structure unit, the central Zn(II) ion is four-coordinated in a distorted tetrahedral environment with two oxygen atoms from two *m*-$FcC_6H_4COO^-$ units and two nitrogen atoms from two bridging bpe ligands. The Zn–O bond length is 1.982(4) Å, and the Zn–N bond length is 2.078(4) Å. The bond angles around Zn1 vary from 94.5(2) to 122.8(3)°. All bpe units connect all Zn(II) ions leading to infinite zigzag chain and neighboring Zn ··· Zn distance is 13.518(2) Å. The one-dimensional

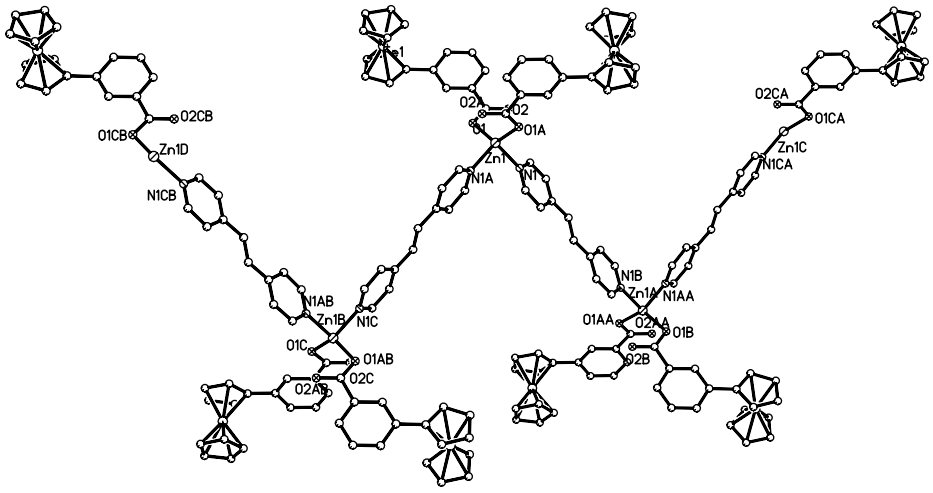

Fig. 2. One-dimensional zigzag chain structure of the polymer $[Zn(OOCH_4C_6Fc)_2(bpe)]_n$.

chains extend along the *c*-direction and pack each other by intermolecular interactions. The structure is similar to the reported 1-D infinite zigzag chain polymer $[Zn(FcCOO)(\eta^2\text{-}FcCOO)(bbp)]_n$ [9b], in which the Zn(II) ions are five-coordinated, and they are in an axially distorted, trigonal bipyriamidal arrangement. The bbp (bbp = 4,4′-trimethylene-dipyridine) units connect all Zn(II) ions leading to a infinite zigzag chain and the neighboring Zn ··· Zn distance is 12.180 Å. In addition, it is noteworthy that the dihedral angle between the phenyl ring's plane and the Cp ring's plane of one *m*-$FcC_6H_4COO^-$ unit is 12.7°.

3.1.3. Crystal structure of $[Mn(\eta^2\text{-}OOCH_4C_6Fc)_2(4,4'\text{-}bpy)]_n$ (3)

Polymer **3** has the similar crystal structure (Fig. 3) and the same space group *C*2/*c* as that of polymer **2**. As can be seen from Fig. 3, the structure consists of a polymeric chain in which adjacent $[Mn(\eta^2\text{-}OOCH_4C_6Fc)_2]$ units are linked by 4,4′-bpy ligands. Each Mn(II) ion is at a six-coordinated geometry in which four oxygen atoms come from two *m*-$FcC_6H_4COO^-$ units, two nitrogen atoms come from two bridging 4,4′-bpy ligands. The Mn-O distances are 2.208(3) and 2.246(2) Å, respectively, while Mn-N distance is 2.246(2) Å. The bond angles around Mn(II) ions range from 58.42(9)° to 145.09(10)°. Interestingly, compared with those of polymers **1** and **2**, *m*-$FcC_6H_4COO^-$ units in polymer **3** as a terminal bidentate fashion coordinate to the central metal ions and hang on the main chains, while in polymers **1** and **2**, *m*-$FcC_6H_4COO^-$ units adopt a tridentate and monodentate fashion, respectively. The center-to-center distance between planes of two parallel phenyl rings of neighboring chains is 7.534 Å. The 4,4′-bpy ligands of neighboring chains are nearly parallel with a dihedral angle of 1.2°, and the center-to-center distance between the two neighboring parallel 4,4′-bpy ligands is 5.419 Å. Since the distances are out of the range of π–π stacking interactions, there are no such interactions in the crystal structure. Moreover, the dihedral angle between the phenyl ring's plane and the Cp ring's plane of one *m*-$FcC_6H_4COO^-$ unit is 15.6°, which is slightly bigger than those of polymers **1** and **2**.

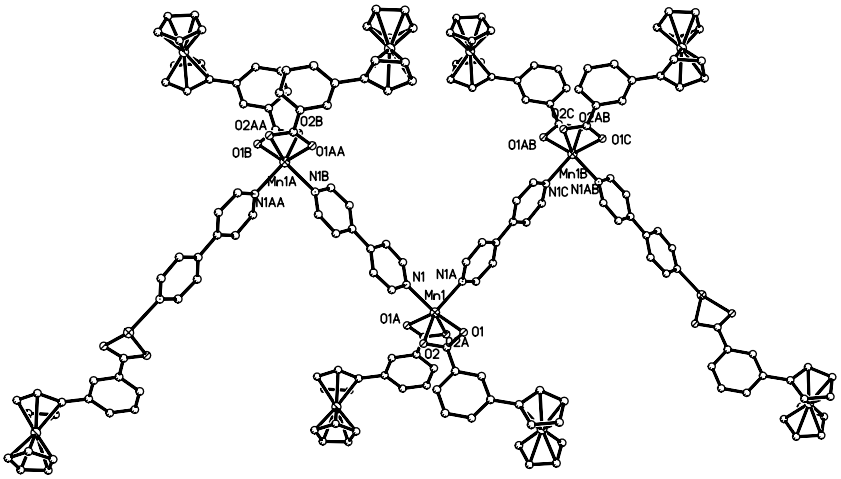

Fig. 3. One-dimensional zigzag chain structure of the polymer $[Mn(\eta^2\text{-}OOCH_4C_6Fc)_2(4,4'\text{-}bpy)]_n$.

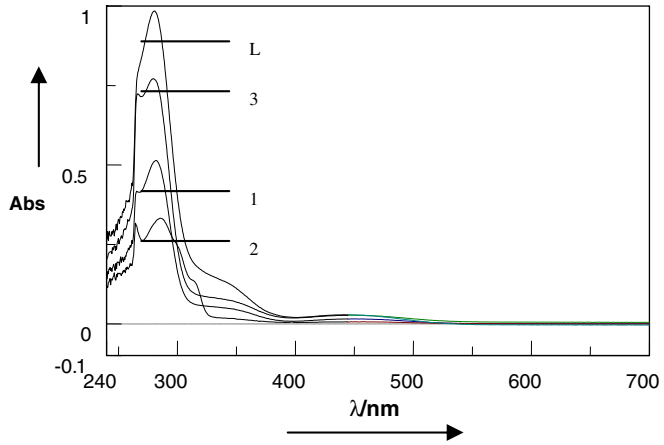

Fig. 4. The UV/Vis spectra of polymers **1**, **2**, **3** and sodium *m*-ferrocenylbenzoate in dilute DMF solution with the maxim of the absorption peaks positioned at 282.0 nm, 285.5 nm, 279.5 nm and 281.0 nm, respectively.

3.2. Nonlinear optical properties

The third-order NLO properties of polymers **1**–**3** were investigated with 532 nm laser pulses of 8 ns duration by *Z*-scan experiment in a 3.78×10^{-4} (**1**), 1.46×10^{-4} (**2**), or 1.52×10^{-4} (**3**) mol dm^{-3} DMF solution. Very low linear absorption in the visible and near-IR regions range from 500 to 700 nm (Fig. 4) promising low-intensity loss and little temperature change caused by photon absorption when light propagates in the materials [18]. This demonstrates that the NLO responses of **1**, **2** and **3** in DMF are neat without the interference of other absorption at the wavelength of 532 nm by the *Z*-scan technique. Polymers **1**–**3** exhibit strong NLO refractive properties (Fig. 5). The third-order NLO studies in DMF solution show that all these polymers display self-focusing behaviors. An effective third-order nonlinear refractive index n_2 can be derived from the difference between normalized transmittance values at valley and peak positions (ΔT_{V-P}) by using Eq. (1) [14,19]:

$$n_2 = \frac{\lambda \alpha_0}{0.812\pi I(1 - e^{-\alpha_0 L})} \Delta T_{V-P} \quad (1)$$

where α_0 is the linear and nonlinear absorption coefficients; L is the sample thickness; λ is the wavelength of the laser; I is the peak irradiation intensity; ΔT_{V-P} is the difference between the normalized transmittance values at valley and peak portions. The n_2 values of polymers **1**–**3** are calculated to be 2.44×10^{-11}, 2.33×10^{-11}, and 2.10×10^{-11} esu,

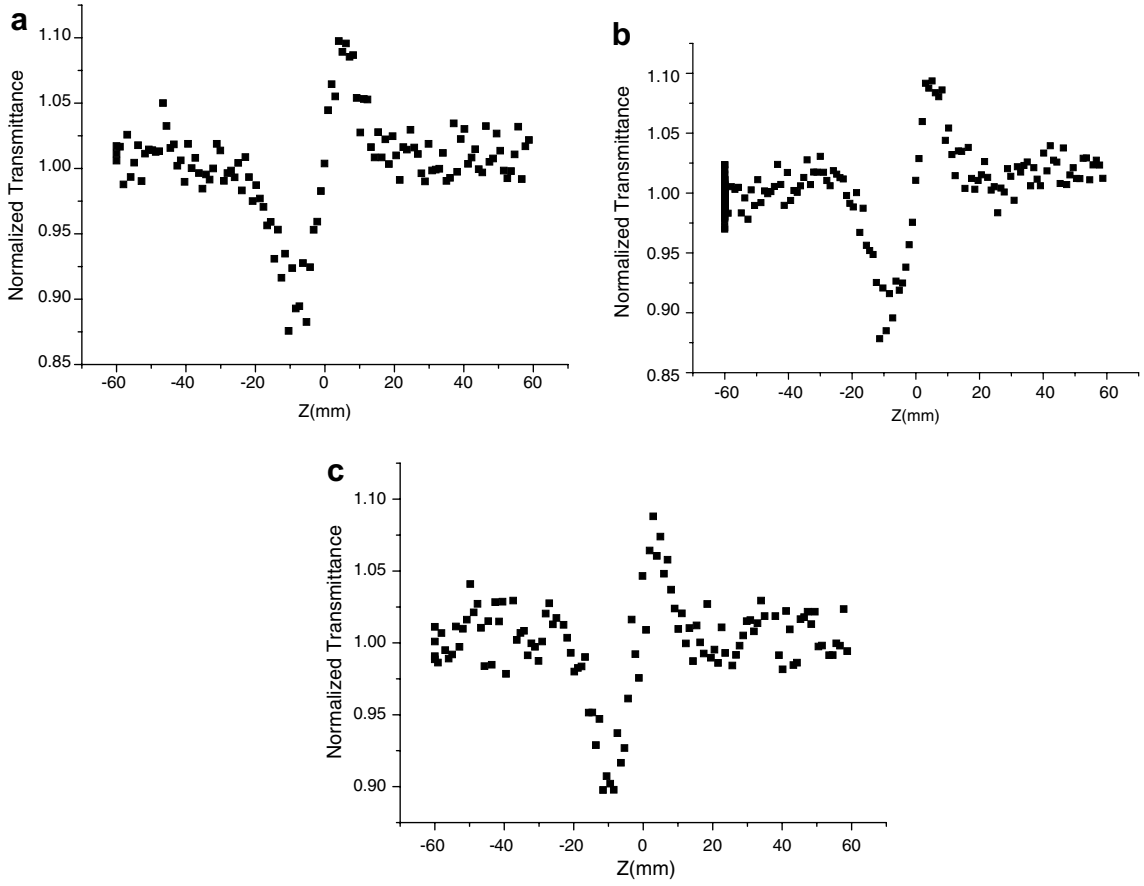

Fig. 5. *Z*-Scan data for **1**–**3**. The data were assessed by dividing the normalized *Z*-scan data obtained in the closed-aperture configuration by the normalized *Z*-scan data obtained in the open-aperture configuration. The black dots are the experimental data. (a) The self-focusing effects of **1** in 3.78×10^{-4} M DMF solution at 532 nm. (b) The self-focusing effects of **2** in 1.46×10^{-4} M DMF solution at 532 nm. (c) The self-focusing effects of **3** in 1.52×10^{-4} M DMF solution at 532 nm.

respectively. In accordance with the n_2 values, the value of third-order NLO susceptibility $\chi^{(3)}$ of the molecule is related to molecular structure. The third-order NLO susceptibility $\chi^{(3)}$ values of polymers **1**, **2** and **3** can be calculated from the equation $\chi^{(3)} = cn_0^2 n_2/80\pi$, where c is the speed of light in a vacuum, and n_0 is the linear refractive index of the sample. The $\chi^{(3)}$ values of polymers **1**–**3** are calculated to be 6.19×10^{-13} esu, 5.9×10^{-13} esu, and 5.3×10^{-13} esu, respectively. The $\chi^{(3)}$ values of polymers **1**, **2**, and **3** are slightly weaker than those of the known cluster compounds (the $\chi^{(3)}$ values are in the range of 10^{-9}–10^{-12}) [20], and can be comparable to those of other ferrocenyl derivatives [21]. A much larger n_2 or $\chi^{(3)}$ value may be expected if a much higher concentration can be achieved.

In order to further investigate the contribution of metal ions and ligands to the delocalization of the π-electron cloud. We used the Gaussian 03 suit of programs to calculate frontier molecular orbitals by density functional theory (DFT) [16,22,23] and analyze orbital occupied components of each part. All DFT calculations were carried out using the B3LYP hybrid exchange-correlation functional [16,22,24]. The basis set used for C, O, N and H atoms was 6-31G(d) [25], while effective core potentials with a LanL2DZ basis set were employed for transition metals and Pb(II) ions [26]. A view of the results is presented in Fig. 6. It can be seen from Fig. 6 that HOMO − 1 and HOMO of polymer **1** are primarily *m*-$FcC_6H_4COO^-$-based orbital (DFT/B3LYP 99.99% and 99.99% for *m*-$FcC_6H_4COO^-$), while LUMO and LUMO + 1 are Pb(II)- and *m*-$FcC_6H_4COO^-$-based orbitals [DFT/B3LYP 69.76% and 52.10% for Pb(II)]. Similarly, the molecular orbitals of polymers **2** and **3** are also calculated. The HOMO − 1 and HOMO of polymer **2** are primarily *m*-$FcC_6H_4COO^-$-based orbital (DFT/B3LYP 99.99% and 99.97% for *m*-$FcC_6H_4COO^-$), while LUMO and LUMO + 1 are bpe-based orbital (DFT/B3LYP 99.74% and 99.54% for bpe), and the four orbitals have barely any Zn(II) character. In polymer **3**, HOMO − 1 and HOMO (Alpha Molecular Orbital) are primarily *m*-$FcC_6H_4COO^-$-based orbital (DFT/B3LYP 98.82% and 81.65% for *m*-$FcC_6H_4COO^-$), HOMO (Beta Molecular Orbital) is primarily Mn(II)-based orbital [DFT/B3LYP 84.17% for Mn(II)], while LUMO and LUMO + 1 are primarily 4,4′-bpy-based orbital [DFT/B3LYP 88.75%, 93.44% (Alpha) and 89.49%, 94.44% (Beta), respectively, for 4,4′-bpy]. Through calculating the components of metal ions and ligands in the frontier molecular orbitals, we can ascertain their contribution to those orbitals. Commonly, the photochemical and photophysical properties of complexes are governed by the first excited singlet state S_1 and the first excited triplet state T_1, which usually associate with the frontier molecular orbitals [27]. The delocalization of the π-electron cloud corresponds to the frontier molecular orbital and such cloud is suggested as the origin of NLO properties of metal complexes, thus the components of the frontier molecular orbitals are very important to NLO properties of complexes. In polymer **1**, both the Pb(II) and *m*-$FcC_6H_4COO^-$ ions contribute to the frontier molecular orbital, accordingly, we can deduce the NLO properties of polymer **1** are controlled by Pb(II) and ferrocenyl ligands, that is to say that Pb(II) ions have some influence on the NLO properties. It is consistent with our former reports [28]. Also we can deduce that the NLO properties of polymer **3** are controlled by ferrocenyl ligands and organic adjuvant ligands, and Mn(II) ions have slightly weak influence on the NLO properties. While in polymer **2**, Zn(II) ions have no influence on the NLO properties, which are only controlled by ferroceneyl ligands and adjuvant ligands. From occupying orbital components of 4,4′-bpy and bpe, the introduction of organic adjuvant ligands involving π-conjugated system have strong influence on NLO properties of polymers. Our recent quantum chemistry studies on NLO properties of Zn(II) complexes [11d,29] also illustrate that the frontier molecular orbitals of Zn(II) complexes primarily have ligands character.

4. Electrochemistry

The solution-state cyclic voltammograms (CVs) and differential pulse voltammograms (DPVs) of **1**–**3** and sodium *m*-ferrocenylbenzoate are shown in Fig. 7. It can be seen from CVs that all these polymers and sodium *m*-ferrocenylbenzoate show a single-electron redox process, which can be assigned to the Fe(II)/Fe(III) couple electron-transfer course of the ferrocenyl moiety. The solution-state DPVs of **1**, **2**, **3** and sodium *m*-ferrocenylbenzoate show a single peak with a half-wave potential ($E_{1/2}$ vs. SCE) at 0.480 V for **1**, 0.472 V for **2**, 0.512 V for **3**, and 0.448 V for sodium *m*-ferrocenylbenzoate. Compared with that of *m*-ferrocenylbenzoate (0.448 V), the half-wave potentials of **1**–**3** are all shifted to slightly higher potential. It is apparent that these shifts can be attributed to the influence of the

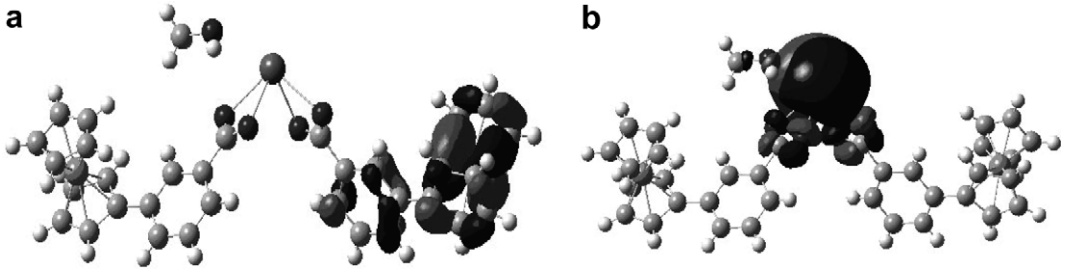

Fig. 6. The frontier molecular orbital of polymer **1**: (a) HOMO, (b) LUMO.

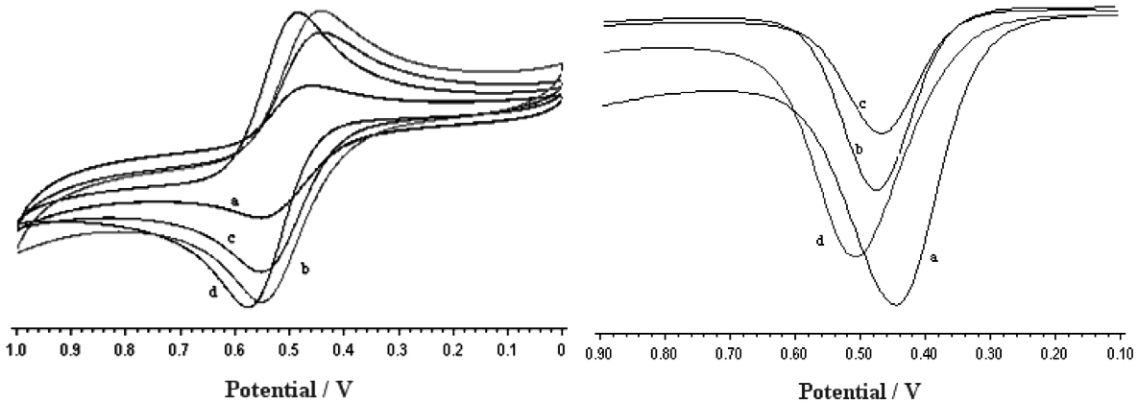

Fig. 7. Cyclic voltammograms (left) and differential pulse voltammograms (right) of polymers **1** (b), **2** (c), **3** (d) and sodium *m*-ferrocenylbenzoate (a) (1.0×10^{-3} M) in DMF solution containing *n*-Bu_4NClO_4 (0.1 M) at a scanning rate of 20 mV s^{-1} (vs. SCE).

central metal ions, and this is consistent with the previous results of transition metal–ferrocenyl systems [30]. The electron-withdrawing nature of the coordinated metal centers will make the ferrocene unit harder to oxidize [31]. Also it should be pointed out that the half-wave potential of the ferrocenyl moiety in **3** has slightly higher value than those of **1** and **2**. We may get an explanation of such behaviors from frontier orbital theory [32]. In **3**, the HOMO orbital is associated with the *m*-$FcC_6H_4COO^-$ and Mn(II) groups, the charge transitions of the metal cores may play an important role in the change of the Fe(II)/Fe(III) oxidation potential of **3**. While the HOMO orbitals in **1** and **2** are located in the *m*-$FcC_6H_4COO^-$ groups, the Fe(II) centers of **1** and **2** are more easily oxidized to Fe(III) centers than that of **3**.

5. Conclusion

In summary, we design and synthesize three new 1-D polymeric complexes, all of which exhibit good third-order NLO properties. By experimental and quantum chemistry study, we conclude that the introduction of organic adjuvant ligands containing π-conjugated system have strong influence on the NLO properties and the nonlinear refractive behaviors of three polymers mainly come of the ferrocenyl units and organic adjuvant ligands; Mn(II) ions and Pb(II) ions have also some influence on NLO properties. In addition, we also elucidate the possible reason for their electrochemical behaviors. Based on molecular orbital calculations we can obtain materials with better photochemical and photophysical properties accurately and easily, and further studies are under way to design particular ferrocenyl complexes with preeminent chemical and physical properties.

Acknowledgement

We gratefully acknowledge the financial support of the National Science Foundation of China (Nos. 20671082 and 20371042).

Appendix A. Supplementary data

Supplementary data associated with this article can be found, in the online version, at doi:10.1016/j.jorganchem.2006.12.010.

References

[1] (a) S. Shi, Z. Lin, Y. Mo, X.Q. Xin, J. Phys. Chem. 100 (1996) 10696;
(b) H.M. Gibbs, Optical Bistability: Controlling Light with Light, Academic, New York, 1985;
(c) B.S. Wherrett, S.D. Smith (Eds.), Optical Bistability: Dynamical Nonlinearity and Photonic Logic, Royal Society, London, 1985;
(d) T.K. Gustafson, P.W. Smith (Eds.), Photonic Switching, Springer, Berlin, 1988;
(e) S.K. Han, Z. Huo, R. Srivastava, R.V. Ramaswamy, J. Opt. Soc. Am. B 6 (1989) 663.
[2] (a) T.S. Wang, Z.L. Ahmadi, T.C. Green, A. Henglein, M.A. Elsayed, Science 272 (1996) 1924;
(b) J.W. Perry, K. Mandour, I.Y.S. Lee, X.L. Wu, P.V. Bedworth, C.T. Chen, D. Ng, S.R. Marder, P. Miles, T. Wada, M. Tian, H. Sasabe, Science 273 (1996) 1533;
(c) J.L. Bredas, C. Adant, P. Tackx, Chem. Rev. 94 (1994) 243.
[3] (a) P. Nguyen, P. Gomez-Elipe, I. Manners, Chem. Rev. 99 (1999) 1515;
(b) N.G. Long, Angew. Chem. Int. Ed. Engl. 34 (1995) 21;
(c) I. Cuadrado, M. Moran, C.M. Casado, B. Alonso, J. Coord. Rev. 395 (1999) 193;
(d) D.A. Davies, J. Silver, G. Cross, P.J. Thomas, J. Organomet. Chem. 631 (2001) 59;
(e) K.N. Jayaprakash, P.C. Ray, I. Matsuoka, M.M. Bhadbhade, V.G. Puranik, P.K. Das, H. Nishihara, A. Sarkar, Organometallics 18 (1999) 3851;
(f) I.S. Lee, H. Seo, Y.K. Chung, Organometallics 18 (1999) 1091;
(g) M.L.H. Green, S.R. Marder, M.E. Thompson, J.A. Bandy, D. Bloor, P.V. Kolinsky, R.J. Jones, Nature 330 (1987) 360.
[4] (a) Y.H. Liu, Y.L. Lu, H.C. Wu, J.C. Wang, K.L. Lu, Inorg. Chem. 41 (2002) 2592;
(b) X. Lei, M. Shang, A. Patil, E.E. Wolf, T.P. Fehlner, Inorg. Chem. 35 (1996) 3217;
(c) G. Baskar, K. Landfester, M. Antonietti, Macromolecules 33 (2000) 9228;
(d) D.N. Hendrickson, S.M.J. Aubin, R.C. Squire, K. Folting, W.E. Streib, G. Christou, Angew. Chem. Int. Ed. Engl. 34 (1995) 887.
[5] G. Li, Y.L. Song, H.W. Hou, L.K. Li, Y.T. Fan, Y. Zhu, X.R. Meng, L.W. Mi, Inorg. Chem. 42 (2003) 913.

[6] (a) T. Wada, L. Wang, H. Okawa, T. Masuda, M. Tabata, M. Wan, M. Kakimoto, Y. Lmai, H. Sasabe, Mol. Cryst. Liq. Cryst. Sci. Technol. Sect. A 294 (1997) 245;
(b) C. Francis, K. White, G. Boyd, R. Moshrefzadeng, Chem. Mater. 5 (1993) 506;
(c) S. Morina, T. Yamashita, K. Horie, T. Wada, H. Sadabe, Rec. Funct. Polymer. 44 (2000) 183;
(d) H.S. Nalwa, Adv. Mater. 5 (1993) 341.
[7] H. Chao, R.H. Li, B.H. Ye, H. Li, X.L. Feng, J.W. Cai, J.Y. Zhou, L.N. Ji, J. Chem. Soc., Dalton Trans. (1999) 3711.
[8] L.K. Li, Y.L. Song, H.W. Hou, Y.T. Fan, Y. Zhu, Eur. J. Inorg. Chem. (2005) 3238.
[9] (a) H.W. Hou, L.K. Li, Y. Zhu, Y.T. Fan, Y.Q. Qiao, Inorg. Chem. 43 (2004) 4767;
(b) H.W. Hou, L.K. Li, G. Li, Y.T. Fan, Y. Zhu, Inorg. Chem. 42 (2003) 3501;
(c) G. Li, H.W. Hou, L.K. Li, X.R. Meng, Y.T. Fan, Y. Zhu, Inorg. Chem. 42 (2003) 4995.
[10] (a) D.C. Rodenberger, J.R. Heflin, A.F. Garito, Nature 359 (1992) 309;
(b) W.F. Sun, M.M. Bader, T. Carvalho, Opt. Commun. 215 (2003) 185.
[11] (a) T.J. Marks, M.A. Ratner, Angew. Chem. Int. Ed. Engl. 34 (1995) 155;
(b) L.R. Dalton, A.W. Harper, R. Ghosn, W.H. Steir, M. Ziari, H. Fetterman, Y. Shi, R.V. Mustacich, A.K.Y. Jen, K.J. Shea, Chem. Mater. 7 (1995) 1060;
(c) R.G. Benning, J. Mater. Chem. 5 (1995) 365;
(d) H.W. Hou, Y.L. Wei, Y.L. Song, L.W. Mi, M.S. Tang, L.K. Li, Y.T. Fan, Angew. Chem. Int. Ed. 44 (2005) 6067.
[12] P. Hu, K.Q. Zhao, L.F. Zhang, J. Si. Chuan, Normal. Univ. (Nat. Sci. Ed.) 21 (4) (1998) 433 (in Chinese).
[13] (a) G.M. Sheldrick, SHELXTL-97, Program for Refining Crystal Structure Refinement, University of Göttingen, Germany, 1997;
(b) G.M. Sheldrick, Acta Crystallogr. Sect. A 46 (1990) 467.
[14] M. Sheik-Bahae, A.A. Said, T.H. Wei, D.J. Hagan, E.W.V. Stryland, IEEE. J. Quantum Electron. 26 (1990) 760.
[15] M.J. Frisch et al., GAUSSIAN03, Revision B.05, Gaussian, Inc., 2003.
[16] A.D. Becke, J. Chem. Phys. 98 (1993) 5648.
[17] (a) X.J. Lei, M.Y. Shang, A. Patil, E.E. Wolf, T.P. Fehlner, Inorg. Chem. 35 (1996) 3217;
(b) P.G. Harrison, A.T. Steel, J. Organomet. Chem. 239 (1982) 105.
[18] Q.F. Zhang, Y.Y. Niu, W.H. Leung, Y.L. Song, I.D. Williams, X.Q. Xin, Chem. Commun. 12 (2001) 1126.
[19] M. Sheik-Bahae, A.A. Said, E.W.V. Stryland, Opt. Lett. 14 (1989) 955.
[20] (a) C. Zhang, Y.L. Song, Y. Xu, G.C. Jin, G.Y. Fang, Y.X. Wang, H.K. Fun, X.Q. Xin, Inorg. Chim. Acta 311 (2000) 25;
(b) H.W. Hou, H.G. Ang, S.G. Ang, Y.T. Fan, M.K.M. Low, W. Ji, Y.W. Lee, Phys. Chem. Chem. Phys. 1 (1999) 3145;
(c) S. Shi, H.W. Hou, X.Q. Xin, J. Phys. Chem. 99 (1995) 4050.
[21] (a) G. Rojo, F. Agulló-López, J.A. Campo, M. Cano, M.C. Lagunas, J.V. Heras, Synth. Met. 124 (2001) 201;
(b) Y.P. Tian, Z.L. Lu, X.Z. You, Acta Chim. Sinica 57 (1999) 1068.
[22] (a) C. Lee, W. Yang, R.G. Parr, Phys. Rev. B 37 (1998) 785;
(b) L.F. Veiros, J. Organomet. Chem. 632 (2001) 3;
(c) M. Pavelka, J.V. Burda, Chem. Phys. 312 (2005) 193;
(d) P.L. Douglas, R.R. Kenton, J. Phys. Chem. B 108 (2004) 13839.
[23] G. Gopi Krishna, R. Sudarshan Reddy, P. Raghunath, K. Bhanuprakash, M. Lakshmi Kantam, B.M. Choudary, J. Phys. Chem. B 108 (2004) 6112.
[24] P.J. Stephens, F.J. Devlin, C.F. Chablowski, M.J. Frisch, J. Phys. Chem. 98 (1994) 11623.
[25] (a) R. Ditchfield, W.J. Hehre, J.A. Pople, J. Chem. Phys. 54 (1971) 724;
(b) W.J. Hehre, R. Ditchfield, J.A. Pople, J. Chem. Phys. 56 (1972) 2257;
(c) P.C. Hariharan, J.A. Pople, Mol. Phys. 27 (1974) 209;
(d) M.S. Gordon, Chem. Phys. Lett. 76 (1980) 163;
(e) P.C. Hariharan, J.A. Pople, Theor. Chim. Acta 28 (1973) 213.
[26] (a) P.J. Hay, W.R. Wadt, J. Chem. Phys. 82 (1985) 299;
(b) T.H. Dunning Jr., P.J. Hay, in: H.F. Schaefer (Ed.), Modern Theoretical Chemistry, III, vol. 3, Plenum Press, New York, 1976, p. 1.
[27] Y. Chen, Y.X. Wang, S. Ye, Int. J. Quantum Chem. 103 (2005) 60.
[28] X.R. Meng, Y.L. Song, H.W. Hou, Y.T. Fan, G. Li, Y. Zhu, Inorg. Chem. 42 (2003) 1306.
[29] J. Wu, Y.L. Song, E.P. Zhang, H.W. Hou, Y.T. Fan, Y. Zhu, Chem. Eur. J. 12 (2006) 5823.
[30] (a) G.L. Zheng, J.F. Ma, Z.M. Su, L.K. Yan, J. Yang, Y.Y. Li, et al., Angew. Chem. Int. Ed. 43 (2004) 2409;
(b) R. Horikoshi, T. Mochida, H. Moriyama, Inorg. Chem. 41 (2002) 3017;
(c) A. Ion, M. Buda, J.C. Moutet, E. Saint-Aman, G. Royal, I. Gautier-Luneau, M. Bonin, R. Ziessel, Eur. J. Inorg. Chem. (2002) 1357;
(d) E.M. Barranco, O. Crespo, M.C. Gimeno, P.G. Jones, A. Laguna, M.D. Villacampa, J. Organomet. Chem. 592 (1999) 258;
(e) Y.M. Xu, P. Saweczko, H.B. Kraatz, J. Organomet. Chem. 637 (2001) 335.
[31] E.M. Barranco, O. Crespo, M.C. Gimeno, P.G. Jones, A. Laguna, C. Sarroca, J. Chem. Soc., Dalton Trans. (2001) 2523.
[32] T. Mitsumori, M. Bendikov, O. Dautel, F. Wudl, T. Shioya, H. Sato, Y. Sato, J. Am. Chem. Soc. 126 (2004) 16793.